Raman Spectroscopy in Coatings Research and Analysis: Part II. Practical Applications

by Neil J. Everall, ICI PLC*

In this two-part tutorial, the use of Raman spectroscopy for characterizing and testing coatings is examined. Part I covered the type of information that can be obtained using Raman spectroscopy (August 2005 JCT CoatingsTech, page 38), and described how a coating is studied in a typical Raman experiment. Part I also discussed the thickness of the coating to be studied, and the influence of the substrate. In this section, we focus on examples that illustrate the capabilities and limitations of Raman spectroscopy.

APPLICATIONS AND EXAMPLES

Compositional Mapping

Perhaps the most obvious application of Raman spectroscopy to coating technology is compositional mapping, whereby a map or image of the composition of a coating can be built up in one, two, or three dimensions. Raman mapping involves sequential acquisition of Raman spectra as a laser beam is incrementally rastered over a sample. An image can then be constructed based upon the intensity (or some other parameter, such as position or width) of a Raman band as a function of position on the sample. (Global) Raman imaging involves defocusing the laser to illuminate a large, 2D area of a sample, and then sequential acquisition of images at distinct Raman frequencies (selected using a tuneable filter). In principle, this is an attractive approach, and for simple, stable systems, where it is only necessary to record images at a few (well-separated) Raman frequencies, it can be very fast. However, if many Raman bands have to be analyzed to understand the coating chemistry, then it can take a long time to acquire images at all of the necessary frequencies. In addition, Raman imaging requires a high power laser beam (to generate a reasonable power density at the sample when the beam is defocused), and it turns out that samples are more prone to thermal decomposition under global illumination than point illumination, due to the difficulty in conducting heat away from a "sheet" of hot material at the sample surface. There are also hybrid technologies available, where the laser is focused to a line on the sample; spectra are acquired simultaneously at each point along the line, using a spectrograph/CCD (Charge-Coupled Device) camera combination, then the line is moved to a new point on the sample. Approaches to Raman mapping and imaging have been summarized in detail elsewhere.[18-20,33]

Many of the examples discussed in this tutorial involve measuring spatial variations in a property, so only a few examples of compositional mapping and imaging will be given here. Roberts and Evans studied the influence of manufacturing variables on the surface quality of paper laminates impregnated with melamine-formaldehyde (MF) and urea-formaldehyde (UF) resins.[34] They used Raman microscopy to map the MF distribution as a function of the amount of UF that was added to the system. They showed that if the UF level was too low, then the MF tended to fill voids in the center of the laminate, leaving the surface MF-deficient and causing visible defects. Increasing the amount of UF prevented ingress of the MF into the body of the laminate, thereby increasing the MF concentration at the surface, giving fewer defects. Larsson et al. used confocal Raman axial profiling with a water-immersion objective to map ligand distributions in surface-treated chromatographic adsorbent particles.[35] They showed how accurate axial profiles of allyl, sulphopropyl, and dextran concentrations could be obtained from particles immersed in water. This proved that the sulphopropyl groups were confined to thin (~20 μm) shells on the surface of 100 μm diameter bead, and allowed coating thickness to be assessed for different particle types. The power of global Raman imaging was shown in a detailed study of the near-surface composition of a thermoplastic olefin (TPO) that was sprayed with a chlorinated polyolefin (CPO) to form a primer layer for subsequent painting.[36] The TPO was a blend of ethylene-propylene rubber (EPR) and poly(propylene) (PP). The Raman image showed separation of the TPO in distinct EPR and PP phases, with the EPR and CPO being co-localized near the surface. The authors suggested that the solvent carrier for the CPO spray was responsible for inducing separation of the TPO into its EPR and PP components. This work also highlighted the need for multivariate data processing to analyze the large volume of data that is generated in spectroscopic images (*Figure* 9).

*Measurement Science Group, The Wilton Centre, Wilton, Redcar, TS104RF, UK.

Crystallinity in Polymeric Coatings

On occasion, one needs to characterize crystallinity gradients in polymer films and coatings. For example, in order to achieve good adhesion between the polyester coatings and metal substrates used in can production, it is important to control the polymer crystallinity so as to retain an amorphous layer near the metal surface, while maintaining a reasonable level of crystallinity elsewhere to avoid compromising the mechanical performance of the coat. The critical changes can occur within just one or two microns of the metal surface, so excellent spatial resolution is required. *Figure* 10 shows a Raman line map, taken at 1 µm increments through a cross-section of a steel-polyester laminate. As one approaches the metal, the crystallinity falls dramatically (decrease in intensity of the 1096 cm^{-1} band over a distance of just 2 µm to yield amorphous polymer at the metal interface). This result confirms that both the coating and the can-forming processes have been controlled to produce an acceptable film structure both in the bulk and at the interface. Similarly, using polarized confocal Raman microscopy, it is possible to map changes in polymer molecular orientation rather than crystallinity, because the intensity of a Raman band depends on the polarization of the laser and Raman fields and the orientation of the scattering unit.[37] We have used this approach to map gradients through the thickness of uniaxially-oriented PET films.[38]

Cure

UV Cure: Raman spectroscopy is ideally suited to studying the cure of reactive C=C groups; *Figure* 11 provides a simple example. In this case, an unsaturated polyester resin was cured using UV light and a cationic initiator, and a microtomed cross-section was then mapped with a Raman microscope to monitor consumption of the C=C groups as a function of distance from the air interface. The cis and trans C=C isomers can be easily distinguished by their stretching frequencies (an advantage over infrared spectroscopy, where the trans band is almost invisible). We can see that the cis isomer is almost fully consumed irrespective of the distance from the air surface, whereas the trans isomer only cures near the surface. The UV light is attenuated as it penetrates into the coating, and this adversely affects the consumption of the trans C=C groups. The cis isomers are apparently more labile, and so cure to completion despite the UV attenuation. The practical conclusion is that one could maximize the cure in this system by increasing the level of cis isomer in the resin. In this example, the UV penetration controlled the cure profile, whereas in radical-initiated systems one often finds that oxygen inhibition inhibits cure near the surface. In such cases, the 1 µm lateral resolution of the Raman microscope can be vital in quantifying significant changes in cure in the top few microns of a sample.[7]

There is extensive literature on studying UV-cure using Raman spectroscopy; only a few examples are quoted here. Schrof et al. combined confocal Raman and confocal laser scanning microscopy (CLSM) to study filler distribution and cure of urethane-acrylate and ester-acrylate resins, although they neglected the effect of spherical aberration on the Raman depth resolution.[39] Kim et al. combined Raman and ATR-FTIR spectroscopy to study the cure of a polyester acrylate to which an acrylate-functionalized poly(dimethylsiloxane) (AF-PDMS) was added, and showed that there was an optimum level of AF-PDMS which resulted in maximum surface cure and hardness.[40] Unfortunately, it was not clear whether the authors could differentiate acrylate functionality in the PDMS from that in the ester-acrylate copolymer. Nichols and colleagues discussed several UV clearcoats in which spectral overlap made it difficult to resolve bands adequately for quantitation.[41] They showed how second derivatives could be used to improve band resolution and permitted quantitative cure profiling. They cut cross-sections and mapped cure at 10 µm intervals through the coat thickness, and compared situations in which cure was limited by either UV penetration (as in *Figure* 8), or by oxygen inhibition. It was claimed that sufficiently high UV dose could overcome O_2 inhibition at the surface, but their spatial resolution (10 µm) was not adequate to resolve any cure gradients which might be present within the first few microns of the coat.

Raman microscopy is pre-eminent for monitoring spatial cure profiles, but cure kinetics can often be measured more easily using IR spectroscopy. For example, real-time IR spectroscopy has been pioneered by Decker for monitoring UV cure on the ms timescale.[42] It would be difficult to obtain adequate spectral quality as rapidly using Raman spectroscopy.

Thermal Cure

In the paint industry, the drying (i.e., room temperature cure) of alkyd resin is a complex process involving cis-trans isomerization, C=C bond migration and crosslinking, and formation of peroxide and hydroperoxide species. While Raman can follow the C=C consumption and O–O production, FTIR is far better suited to detecting O–O–H production. Claybourn et al. have used Raman and FTIR spectroscopy to follow the drying process in the bulk of paint films and model systems, and observed features such as cis-trans isomerization and the effect of TiO_2 filler on the rate of cure.[43,44] Mirone et al. used confocal Raman to depth profile the cure of C=C in alkyd films, and monitored the dry-

Figure 9—Near-surface distribution of poly(propylene), ethylene-propylene rubber, and chlorinated polyolefin components, in a CPO-sprayed thermoplastic olefin, as visualized using global Raman imaging. Adapted from Figure 9 of reference 36, with permission of The American Chemical Society.

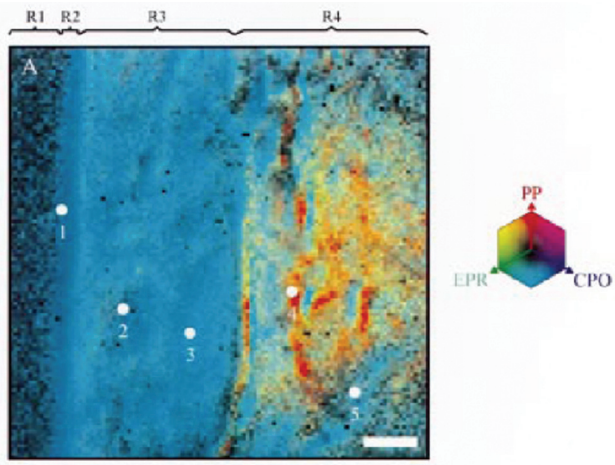

ing front as it moved into the film.[45] The data was used to develop a model to predict the degree of crosslinking and Young's Modulus as a function of film thickness and drying time. Erich et al. combined NMR imaging and confocal Raman microscopy to monitor the penetration of drying fronts into alkyd films.[46] The NMR data were used to calibrate the true sampling depth of the Raman probe, which was shown to be about 1.6 times deeper than the nominal focal point. This confirmed that refraction must be accounted for to correctly analyze the position of the drying front.

Perhaps surprisingly, it is also possible to use Raman spectroscopy to predict the viscosity of paint emulsions. Ito et al. used partial least squares (PLS) regression to predict viscosity over the range 20–350 mPaS with a precision of about 25 mPaS.[47] The model used spectral features relating to chain length and styrene content which had positive and negative correlations with viscosity. Combined with the more obvious measurements of composition and extent of polymerization,[44] this could be an interesting tool for on-line analysis and production control, particularly given the ease with which Raman spectrometers can be configured for process analysis.[48]

Despite Raman spectroscopy's advantages in terms of sampling and spatial resolution, sometimes the basis spectroscopy of the system dictates that IR spectroscopy is the preferred approach. For example, isocyanates are common components of coating materials which cure by reaction with alcohols or water to form urethane (–NCOO–) and urea linkages. Cure of NCO is easily monitored using IR spectroscopy (loss of antisymmetric stretching band near 2280 cm^{-1}), but this band is completely invisible in the Raman spectrum (*Figure* 12). The symmetric NCO stretch, which *is* Raman active, falls at lower frequency and is often masked or overlapped by other bands, notably the amide II (coupled NH bend and CN stretch) bands of the urethane and urea groups that are formed during cure, so it is much harder to locate and quantify. In simple cases, one can still quantify the cure with this peak,[49] but in situations where the urethane is present in both H-bonded and non H-bonded forms there are multiple overlapping spectral features and quantification becomes very difficult. Hence, quantification of NCO cure is usually far more straightforward using IR spectroscopy. In other cases, there is little spectroscopic reason for preferring IR or Raman spectroscopy over the alternative, and either technique can be used. The cure of epoxies is a good example, since the oxirane ring has strong bands in both the IR and Raman. Here, the choice of technique might depend on other factors, such as whether remote sampling is required (e.g., fiber-optic coupled), or whether another component masks the IR or Raman band of interest.

Most cure examples involve fairly straightforward monitoring of simple functional groups with easily assigned group frequencies, but more complicated examples have appeared. Scheepers et al.[50] studied the cure of melamine formaldehyde in water using Raman spectroscopy coupled with NMR and HPLC. Ab-initio calculations of vibrational frequencies enabled confident assignment of bands to monitor the consumption of methylol groups (CH_2–OH), and the generation of crosslinks from methylene (–NH–CH_2–NH– and O–CH_2–OH) and methylene ether (NH–CH_2–O–CH_2–NH–) groups. This was an excellent demonstration of how detailed cure chemistries can be studied.

Figure 10—Crystallinity line-map through poly(ester) coating on steel substrate. Sample prepared by sectioning with diamond-blade. Note decrease in crystallinity band (dashed) near interface. Band near 1000 cm^{-1} is due to additive used to control crystallinity.

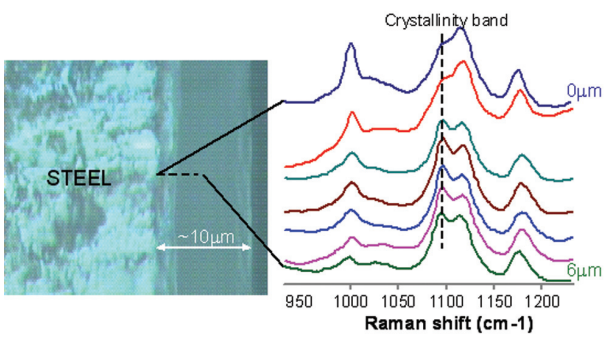

Sol-Gel

Sol-gel processes have been extensively studied with Raman spectroscopy, particularly for hybrid systems where it might be necessary to monitor the cure of a number of individual reactive groups in conjunction with the formation of both organic and inorganic networks. Posset et al. investigated the UV cure of a formulation containing vinyl triethoxysilane and tetra-ethoxysilane, with additional vinyl and acrylate components.[51] They followed the hydrolysis of the alkoxysilane and the crosslinking of the acrylate and vinyl groups, and correlated the degree of crosslinking with the surface hardness before and after weathering. In a more detailed example, Davis et al. used a combination of Raman spectroscopy with $^{29}Si/^{13}C$ NMR spectroscopy to study the polymerization of an epoxy-functionalized alkoxysilane (glycidoxypropyltrimethoxy-silane, or GPTMS).[52] Cure was initiated with an amine agent that can catalyze both ring-opening of the epoxy and condensation of the silanol groups that result from hydrolysis of the methoxysilane species. The GPTMS was dissolved in water and the amine was added, and then the liquid was cast onto a steel substrate, dried at room temperature, and then cured at 150°C for an hour. The GPTMS:amine ratio was varied systematically to investigate the effect on the cure chemistry. The Raman data proved that for high levels of cure agent, extensive ring-opening of the epoxy had occurred after drying (significant loss of 1256 cm^{-1} band), the alkoxysilanes had completely hydrolyzed (loss of 613 and 643 cm^{-1} bands), and a substantial silicate network had formed (broad features near 480 cm^{-1}). Subsequent heating did not significantly advance the loss of epoxy or the generation of silicate, despite the presence of uncured epoxy rings. This implies that the amine rapidly catalyzed the formation of a rigid network that then prevented further consumption of epoxy groups on heating. Reducing the level of amine resulted in a smaller initial consumption of epoxy rings and a less rigid organic network. This is a very nice example of how both the organic and inorganic components of a hybrid system can be monitored with Raman scattering. The ^{29}Si NMR results proved that the average silicate coordination number was higher for samples cured with lower concentrations of amine, and supported the conclusions drawn from the Raman work.

FIBERS/COMPOSITES

The interface between a fiber and the surrounding matrix plays a crucial role in the performance of fiber-reinforced composites. Glass fibers are usually sized (often with a silane) to improve fiber wetting and adhesion. Shih and Koenig carried out a fairly detailed analysis of the spectra of eight different silane coupling agents, and were able to directly observe their reaction and adsorption on glass fiber bundles.[53] The resultant spectra were actually quite strong, but no indication was given as to the thickness of the silane layers. Ishida et al. were able to observe sub-monolayers of silane on glass, but this was a somewhat artificial example using a molecule that contained a phthallocyanine ring.[54] UV laser excitation generated a strongly resonance-enhanced Raman spectrum and allowed submonolayer detection, but the resultant spectrum contained only vibrations due to the chromophore, so only indirect information on the interaction with the glass was obtained. (Resonant Raman scattering occurs when the laser excitation wavelength falls near or within an electronic absorption band of the sample; under these conditions one can observe several orders of magnitude enhancement in the Raman bands of the chromophore). In another example of this effect, Li et al. showed how very thin (~5 nm) coatings of PEEK [poly(aryl-ether-ether-ketone)] could be detected on carbon-fibers using 1064 nm excited Raman spectroscopy.[55] Normally this would be far too thin a layer for detection by FT-Raman spectroscopy, particularly on a highly absorbing substrate, but the authors postulated a strong electronic interaction between the PEEK aryl rings and the carbon fiber, which activated formerly forbidden bands in the Raman spectrum. Presumably this interaction resulted in an electronic absorption near 1064 nm that causes strong resonance enhancement of the PEEK signal. It remains to be seen whether this is a generally-applicable approach for the study of carbon-fiber reinforced composites.

In some cases, one needs to study the fiber-resin interface in the presence of thick overlayers of resin. This can be achieved if the spectrum of the interface is much more intense than in the bulk. For example, Young et al. have used resonance Raman spectroscopy to analyze stress-transfer in glass-fiber reinforced epoxy composites.[56] Prior to forming the composite, the fibers were coated with a diacetylene-containing urethane copolymer that was then cross-polymerized to yield a conjugated system of alternating double and triple bonds. This conjugated system gives very strong, resonant-enhanced Raman bands which show significant frequency shifts under applied stress. This allows the stress to be monitored as a function of position on the discontinuous fibers, which in turn gives information on the adhesion between the resin and the fibers.

Finally, we note that analysis of sizing solutions before and after fiber treatment is a generally applicable approach, since it does not rely on either coincidental or engineered conditions for resonant enhancement of Raman signals. As an example, Norstrom et al. analyzed silane solutions before and after washing E-glass fibers, and were able to analyze both hydrolysis of the silane, and the loss of silane from solution due to uptake by the fibers.[57] This does not give us direct information on the fiber surface chemistry, but it could be an important tool for monitoring the fiber sizing process.

Figure 11—Line-mapping cis and trans double bond consumption in UV-cured unsaturated poly(ester). Note the rapid decrease in trans C=C consumption on moving below the air surface, due to attenuation of the UV. The cis groups are more labile and cure more extensively irrespective of the UV intensity.

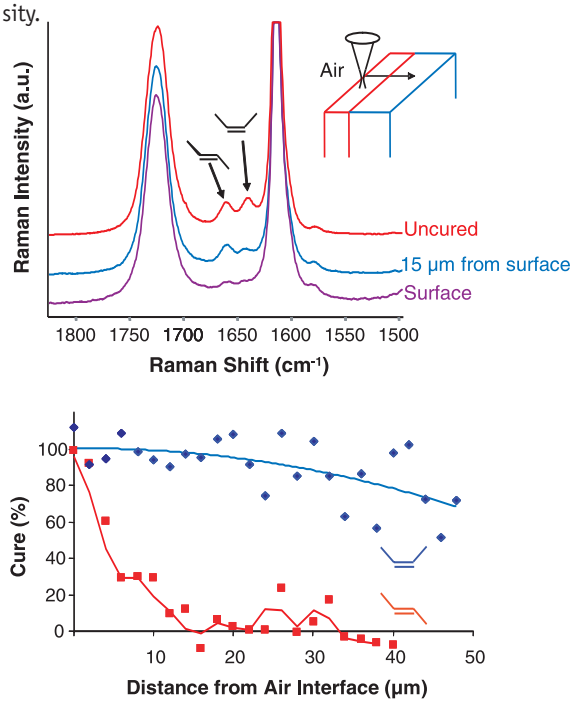

CARBON

Raman spectroscopy is extremely sensitive to the different structures that elemental carbon can assume, and, as such, it is one of the most widely used tools in its study, in forms ranging from amorphous carbon to nanotubes. In coating technology, diamond-like carbon (DLC) coatings, and polycrystalline diamond coatings, are hard, chemically inert, and bio-compatible, with applications ranging from semiconductors to bio-implants. Raman is useful for their characterization since it can distinguish sp^2 and sp^3 hybrids, and give information on the size of nanocrystalline domains.[58] The Raman characterization of carbon coatings is a huge field; in a literature search utilizing the terms "Raman" and "Coating," well over half of the 600 or so references produced pertained to DLC!

As well as being directly deposited, carbon can be formed as a by-product of other processes—for example, ion-implantation of plastic,[59,60] heat treatment of sol-gels,[61] and thermal annealing of metal-carbide ceramics,[62] to name but three. Raman spectroscopy is an invaluable tool for characterizing the carbon by-products of these and similar processes.

CORROSION SCIENCE

Raman spectroscopy can be readily applied to study corrosion in-situ. Bernard et al. used Raman microscopy to study the corrosion of iron that was protected with an epoxy-amine varnish.[63] Here the ability to focus through the overcoat onto the iron surface was critically important, avoiding possible perturbation of the surface through removal of the coating. Also, Raman spectroscopy is well suited to detection of specific crystal forms of inorganics. Consequently, the authors

Figure 12—Comparison of IR and Raman spectra of a polyurethane prepolymer based on methylene-diisocyanate reacted with a polyol. The NCO:OH ratio was 2:1, so as to leave an excess of unreacted NCO groups. The asymmetric NCO stretch is strong in the IR but invisible in the Raman. The symmetric NCO band is visible in the Raman (~1525 cm^{-1}) but is heavily overlapped by the amide II band of urethane and urea groups. Samples kindly provided by M. Diaz, ICI PLC.

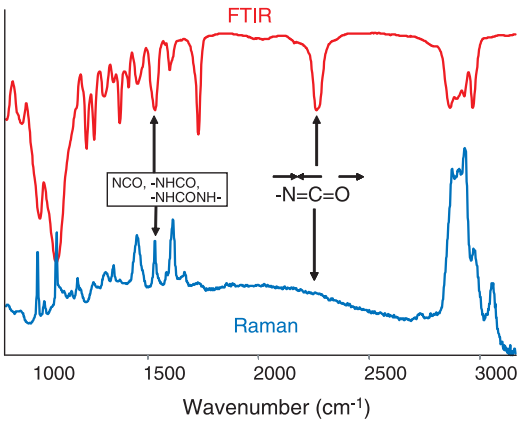

were able to detect the formation of elemental sulphur, αFeOOH (goethite), FeS_2 and αFe_2O_3, after bubbling H_2S through a salt solution in which a coated steel coupon was immersed. Bubbling CO_2 resulted in the formation of iron carbonate. Impedance spectroscopy showed that the films were intact (no ionic diffusion), implying that transport occurs by molecular diffusion through polymer interstices, rather than via macroscopic defects. Le et al. studied electropolymerized polypyrrole films as protective coatings on iron.[64] Not only did this work allow the redox state of the protective coating to be characterized, the corrosion products at the solution/film interface were identified. Tomandl et al. studied the alkaline dissolution of phosphate layers on zinc-coated steel using in-situ Raman spectroscopy.[65] They showed how the presence of Mn can passivate the zinc phosphate layer via formation of manganese hydroxide, conveying greater protection than monocation zinc phosphate.

INORGANICS

Raman spectroscopy is often superior to IR analysis for speciation of inorganics. Raman spectra tend to be sharper than in the IR, making subtle changes in peak position easily visible, and Raman spectrometers give easy access to low frequency modes (0–400 cm^{-1}), which are critical for differentiating crystal forms. For example, exact measurement of the carbonate Raman stretching frequency near 1080 cm^{-1} gives a good indication of the counter ion that is present, or a strong band near 142 cm^{-1} allows detection of sub percent levels of anatase that would be missed by FTIR analysis. Some useful, albeit small, collections of inorganic reference spectra have appeared to aid identifica-tion.[66,67] Numerous electronic collections are available with free access and can be located with simple searches on the World Wide Web (see, for example, http://www.nuigalway.ie/chem/AlanR/ARyderP9.html#9B for useful links to numerous collections).

Perhaps surprisingly, Raman spectra can be very sensitive to crystal size.[68] The sensitivity is highest for nanophase materials, where small changes in crystal diameter give a large change in the surface/volume ratio. As an example, Werninghaus and colleagues applied micro-Raman spectroscopy to characterize cubic boron-nitride (c-BN) thin films deposited onto Si(100).[69] Prior measurements on c-BN crystals of known size established the relationship between position and asymmetry of the ~1260 cm^{-1} Raman band, and the approximate crystal size. The average crystallite size in the film was ~1.3 nm (although strictly speaking, as the authors pointed out, this is the average distance between lattice defects, rather than a true crystal size). The authors were also able to map damage and stress at the silicon surface by measuring the frequency and shape of the silicon phonon near 520 cm^{-1}, and related this to the state of the c-BN overlayer.

Raman spectroscopy is ideal for following phase transitions as a function of temperature. Djaoued et al. deposited brookite-rich titania films onto glass substrates by a sol-gel process, and then monitored the phase composition and crystal size as the temperature was ramped up to 900°C.[70] At temperatures below 600°C, nanophase brookite dominated. Anatase was the dominant phase between 700–800°C, with significant crystal growth occurring in this regime, while at 900°C the system adopted the pure rutile phase. These changes were irreversible. Surface coatings on biomedical implants are amenable to macro and micro Raman characterization, as exemplified by the study of the hydroxyapatite (HA) coatings which are added to improve the biocompatibility of titanium implants. Darimont et al. used confocal Raman microscopy to map the phase structure in plasma-sprayed implants as one moves from the "bulk" coating towards the titanium substrate.[71] They identified two phases—HA, and β-tricalcium phosphate (TCP)— in the coating, with the TCP/HA ratio increasing towards the metal surface. This was attributed to differential cooling rates, with fast cooling at the metal favoring the TCP structure. Because the TCP is acid-soluble, it is bio-active and can be reabsorbed (an undesirable effect since it weakens the joint). Hence, Raman microscopy allows one to adjust the plasma-deposition to produce a thick-enough layer of HA to prevent reabsorption of the underlying TCP. Raman measurements were ideal for this study since they can differentiate these materials quite easily compared with X-ray diffraction (XRD) or FTIR, and the spatial resolution of confocal Raman is well-matched to the morphology of the system.

We have already discussed how Raman bandshifts can be used to measure stress in organic materials, but the same is true of inorganics. Portinha et al. measured residual stresses in thermal barrier coatings (ZrO_2 doped with Y_2O_3) on iron, using Raman and XRD.[72] They analyzed samples after spraying, thermal-shock at 1000°C, and annealing at 1100°C. The authors mapped the stress distribution through the coat thickness using the shift in position of the 640 cm^{-1} zirconia band. Prior calibration showed a linear relationship between band shift and applied stress, with a gradient of 220 MPa per cm^{-1}.[73] They found a compressive stress at the zirconia/iron interface, and a tensile stress at the air surface. The compressive stresses increased after annealing.

THIN COATINGS ON METALS

Under certain conditions, the Raman spectra of molecules near the surface of roughened metals can be massively enhanced in a process known as surface enhanced Raman scattering, or SERS.

The enhancement can be very large, (10^4–10^6), and arises from a large increase in the electric field strength near the metal surface (up to 10^4), coupled with a chemical enhancement due to a charge-transfer interaction between the adsorbate and the metal. For strong SERS, one needs a noble metal substrate, (silver and gold being the most common choices), which has a surface roughness on the 10–100 nm scale, laser excitation at a wavelength that excites a collective electronic oscillation in the metal (a surface plasmon), and adsorption of the analyte molecules onto the metal surface. Under optimum conditions, submonolayer coverage yields strong SERS spectra. A detailed discussion of the SERS mechanism is beyond the scope of this tutorial; the reader is referred to other review articles for more detail.[74,75] Despite its sensitivity, SERS is not widely applicable as a routine analytical tool. First, not all metals and analytes give strong SERS spectra. Second, the SERS spectrum can look very different to the normal Raman spectrum (selective band enhancement, activation of new bands, molecular orientation effects at the surface), making interpretation difficult. Third, the metal-adsorbate complex can be highly reactive, photolyzing in the laser beam to give a range of products. Fourth, the scale of the roughness needs to be carefully controlled to give reproducible results.

From a coating technology viewpoint, SERS is most applicable if one is interested in a coating on a noble metal. This situation does arise, for example, in the development of anticorrosion coatings for copper, where the electrodeposition of benzotriazole and its derivatives onto copper is of great interest.[76-78] However, in principle, one can use SERS to detect and analyze thin coatings on *any* substrate, using the configuration shown in *Figure* 13. For example, we tried to use SERS to detect 10 nm acrylic coatings on PET film, by depositing a thin (~5 nm) silver film on top of the coating, and then focusing the laser beam onto the silver and collecting the Raman scatter through it.[79] Uncoated PET gave a very strong SERS spectrum, but the acrylic coating was only weakly SERS active, so its spectral quality was poor. However, the presence of a coating was sufficient to completely block generation of SERS from the PET. So, although little information on the coating itself was obtained, we could infer the presence of the coating by the absence of a PET SERS spectrum. This could provide a simple method for mapping coat continuity. Without the silver overlayer, one can only observe PET bands irrespective of the presence or absence of the acrylic coating.

With modern instruments it is possible to detect monolayer coatings on smooth metal substrates in the absence of any SERS enhancement. The spectra are much weaker than with SERS, but they are more stable and more readily interpreted. For optimum signal strength, one needs to control the angle of incidence of the laser beam and the angle of collection of the Raman scatter. Campion has summarized the effect of varying the incident and collection angle, and the polarization, on the detected Raman signal.[80] According to this analysis, using incident and collection angles of approximately 60° can boost the Raman signal by about an order of magnitude. Excitation using a Raman microscope with a high numerical aperture objective will excite and collect radiation with a wide range of angles, so it is not optimized for detecting thin layers on metals.

Figure 13—Possible configuration for obtaining SERS spectra of any coating on any substrate. If the coating is SERS active, then by depositing a thin (~10 nm) silver film onto the coating, one can generate SERS spectra by focusing the laser beam onto the silver.

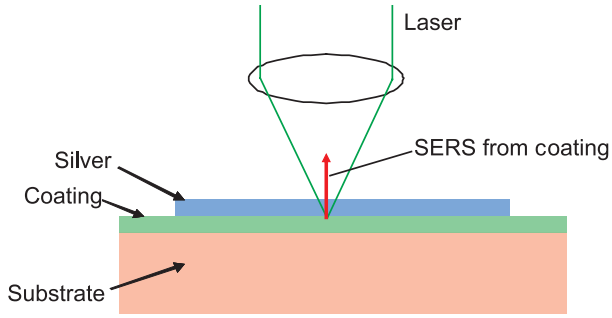

CONCLUSIONS

This tutorial has attempted to illustrate the ways in which Raman spectroscopy can contribute to the study of coatings. An article of this length can only give a flavor for the possibilities, but hopefully the examples given and the literature cited will give a broad indication of what can be achieved. This discussion is far from exhaustive, and a number of exciting technologies (such as sum-frequency generation and near-field Raman microscopy) have been omitted simply on the grounds of space considerations and a current lack of general applicability in the coatings field. CT

References

(1) Chalmers, J.M., "Infrared Spectroscopy in the Analysis, Characterization, and Testing of Coatings," *JCT CoatingsTech*, 2, No. 18, 50 (2005).
(2) Cotton, F.A., *Chemical Applications of Group Theory*, John Wiley and Sons, New York, 1990.
(3) Fateley, W.G., Dollish, F.R., McDevitt, N.T., and Bentley, F.F., *IR and Raman Selection Rules for Molecular and Lattice Vibrations*, Wiley Interscience, New York, 1972.
(4) Mayo, D.W., Miller, F.A., and Hannah, R.W., *Course Notes on the Interpretation of IR and Raman Spectra*, Wiley-Interscience, New York, 2004.
(5) Lin-Vien, D., Colthup, N.B., Fateley, W.G., and Grasselli, J.G., *Handbook of IR and Raman Characteristic Group Frequencies*, Academic Press, New York, 1991.
(6) Socrates, G., *IR and Raman Characteristic Group Frequencies,* 3rd Ed., John Wiley and Sons, Chichester, 2001.
(7) Everall, N.J., in *Analytical Applications of Raman Spectroscopy*, Pelletier, M.J. (Ed.), Blackwell Science, Oxford, pp. 127-192, 1999.
(8) Wang, C., Vickers, T.J., Schlenoff, J.B., and Mann, C.K., *Appl. Spectrosc.* 46, 1729 (1992).
(9) Everall, N., Tayler, P., Chalmers, P., Mackerron, D., Ferwerda, R., and van der Maas, J.H., *Polymer*, 35, 3184 (1994).
(10) Williams, K.J.P. and Everall, N.J., *J. Raman. Spectrosc.*, 26, 427 (1995).
(11) Vickers, T.J. and Mann, C.K., in *Analytical Raman Spectroscopy*, Grasselli, J.G. and Bulkin, B.J. (Eds.), John Wiley and Sons, New York, 1991.
(12) Adar, F. and Noether, H., *Polymer*, 26, 1935 (1985).
(13) Zerbi, G., Ciampelli, F., and Zamboni, V., *J. Polym. Sci. C.*, 141 (1964).
(14) Kawata, S. and Inouye, Y., in *Handbook of Vibrational Spectroscopy,* Vol. 2, Chalmers, J.M. and Griffiths, P.R. (Eds.), John Wiley and Sons, Chichester, pp. 1460-1471, 2002.
(15) Lewis, I.R. and Lewis, M.R., in *Handbook of Vibrational Spectroscopy,* Vol. 2, Chalmers, J.M. and Griffiths, P.R. (Eds.), John Wiley and Sons, Chichester, pp. 1587-1597, 2002.

(16) Greene, P.R. and Bain, C.D., *Spectroscopy Europe*, 16, 8 (2004).
(17) Pelletier, M.J., in *Analytical Applications of Raman Spectroscopy*, Pelletier, M.J. (Ed.), Blackwell Science, Oxford, pp. 53-105, 1999.
(18) *Raman Microscopy: Developments and Applications*, Turrell, G. and Corset, J. (Eds.), Academic Press, New York, 1996.
(19) Dhamelincourt, P., in *Handbook of Vibrational Spectroscopy, Vol. 2*, Chalmers, J.M. and Griffiths, P.R. (Eds.), John Wiley and Sons, Chichester, pp. 1419-1428, 2002.
(20) Treado, P.J. and Nelson, P., in *Handbook of Vibrational Spectroscopy, Vol. 2*, Chalmers, J.M. and Griffiths, P.R. (Eds.), John Wiley and Sons, Chichester, pp. 1429-1459, 2002.
(21) Tabaksblat, R., Meier, R., and Kip, B.J., *Appl. Spectrosc.*, 46, 60 (1992).
(22) Everall, N.J., *Appl. Spectrosc.*, 54, 1515 (2000).
(23) Everall, N.J., *Appl. Spectrosc.*, 54, 773 (2000).
(24) Baldwin, J.K. and Batchelder, D.N., *Appl. Spectrosc.*, 55, 517 (2001).
(25) Froud, C.A., Hayward, I.P., and Laven, J., *Appl. Spectrosc.*, 57, 1468 (2003).
(26) Adar, F., Naudin, C., Whitley, A., and Bodnar, R., *Appl. Spectrosc.*, 58, 1136 (2004).
(27) Everall, N.J., *Spectroscopy* 19, 22 (2004).
(28) Everall, N.J., *Spectroscopy* 19, 16 (2004).
(29) Vyorykka, J., Halttunen, M., Litti, H., Tenhunen, J., Vuorinen, T., and Stenius, P., *Appl. Spectrosc.*, 56, 1123 (2002).
(30) Reinecke, H., Spells, S.J., Sacristan, J., Yarwood, J., and Mijangos, C., *Appl. Spectrosc.*, 55, 1660 (2001).
(31) Ikeshoji, T., Ono, Y., and Mizuno, T., *Appl. Opt.*, 12, 2236 (1973).
(32) Bain, C.D., MacMillan, C., and Everall, N., unpublished data, 2004.
(33) Dahlgren, S.D., Thomas, M.T., Beauchamp, R.H., and Courtright, E.L., *Thin Solid Films*, 119, 365 (1984).
(34) Roberts, R.J. and Evans, P.D., *Compos. Part A: Appl. Sci.*, 36, 95 (2005).
(35) Larsson, M., Lindgren, J., Ljunglof, A., and Knuuttila, K.-G., *Appl. Spectrosc.*, 57, 251 (2003).
(36) Morris, H.R., Turner, J.F., Munro, B., Tryntz, R.A., and Treado, P.J., *Langmuir*, 15, 2961 (1999).
(37) Ikeda, R., Chase, D.B., and Everall, N.J., in *Handbook of Vibrational Spectroscopy*, Vol. 2, Chalmers, J.M. and Griffiths, P.R. (Eds.), John Wiley and Sons, Chichester, pp. 716-730, 2002.
(38) Everall, N.J., *Appl. Spectrosc.*, 52, 1498 (1998).
(39) Schrof, W., Beck, E., Etzrodt, G., Hintze-Bruning, H., Meisenburg, U., Schwalm, R., and Warming, J., *Prog. Org. Coat.*, 43, 1 (2001).
(40) Kim, H.K., Ju, H.T., and Hong, J.W., *Eur. Polym. J.*, 39, 2235 (2003).
(41) Nichols, M.E., Seubert, C.M., Weber, W.H., and Gerlock, J.L., *Prog. Org. Coat.*, 43, 226 (2001).
(42) Decker, C. and Bianchi, C., *Polym. Int.*, 52, 722 (2003).
(43) Agbenyega, J.K., Claybourn, M., and Ellis, G., *Spectrochim. Acta*, A-M, 47, 1375 (1991).
(44) Ellis, G., Claybourn, M., and Richards, S.E., *Spectrochim. Acta*, A-M, 46, 227 (1990).
(45) Mirone, G., Marton, B., and Vancso, G.J., *Eur. Polym. J.*, 40, 549 (2004).
(46) Erich, S.J.F., Laven, J., Pel, L., Huinink, H.P., and Kopinga, K., *Prog. Org. Coat.*, 52, 210 (2005).
(47) Ito, K., Kato, T., and Ona, T., *Vib. Spectosc.*, 35, 159 (2004).
(48) Everall, N., Clegg, I., and King, B., in *Handbook of Vibrational Spectroscopy*, Vol. 4, Chalmers, J.M. and Griffiiths, P.R. (Eds.), John Wiley and Sons, Chichester, pp. 2770-2801, 2002.
(49) Parnell, S., Min, K., and Cakmak, M., *Polymer*, 44, 5137 (2003).
(50) Scheepers, M.L., Gelan, J.M., Carleer, R.A., Adriaensens, P.J., Vanderzande, D.J., Kip, B.J., and Brandts, P.M., *Vib. Spectosc.*, 6, 55 (1993).
(51) Posset, U., Gigant, K., Schottner, G., Baia, L., and Popp, J., *Opt. Mater.*, 26, 173 (2004).
(52) Davis, S.R., Brough, A.R., and Atkinson, A., *J. Non-Cryst. Solids*, 315, 197 (2003).
(53) Shih, P.T.K. and Koenig, J.L., *Mater. Sci. Eng.*, 20, 145 (1975).
(54) Ishida, H., Koenig, J.L., Asumoto, B., and Kenney, M.E., *Polym. Compos.*, 2, 75 (1981).
(55) Li, T.Q., Zhang, M.Q., and Zeng, H.M., *Polymer*, 40, 4307 (1999).
(56) Young, R.J., Thongpin, C., Stanford, J.L., and Lovell, P.A., *Compos. Part A: Appl. Sci.*, 32, 253 (2001).
(57) Norstrom, A., Watson, H., Engstrom, B., and Rosenholm, J., *Colloids Surf., A*, 194, 143 (2001).
(58) Dresselhaus, M.S., Dresselhaus, G., Pimenta, M.A., and Eklund, P.C., in *Analytical Applications of Raman Spectroscopy*, Pelletier, M.J. (Ed.), Blackwell Science, Oxford, pp. 367-434, 1999.
(59) Guzman, L., Miotello, A., Voltolini, E., and Adami, M., *Thin Solid Films*, 377-378, 760 (2000).
(60) Guzman, L., Man, B.Y., Miotello, A., Adami, M., and Ossi, P.M., *Thin Solid Films*, 420-421, 565 (2002).
(61) Que, W., Sun, Z., Zhou, Y., Lam, Y.L., Cheng, S.D., Chan, Y.C., and Kam, C.H., *Mater. Lett.*, 42, 326 (2000).
(62) Zhang, L. and Koka, R.V., *Mater. Chem. Phys.*, 57, 23 (1998).
(63) Bernard, M.C., Duval, S., Joiret, S., Keddam, M., Ropital, F., and Takenouti, H., *Prog. Org. Coat.*, 45, 399 (2002).
(64) Nguyen Thi Le, H., Bernard, M.C., Garcia-Renaud, B., and Deslouis, C., *Synth. Met.*, 140, 287 (2004).
(65) Tomandl, A., Wolpers, M., and Ogle, K., *Corros. Sci.*, 46, 997 (2004).
(66) Burgio, L. and Clarke, R.J.H., *Spectrochim. Acta*, 57A, 1491 (2001).
(67) Degen, I.A. and Newman, G., *Spectrochim. Acta*, 49A, 859 (1993).
(68) Everall, N.J., in *Handbook of Vibrational Spectroscopy*, Vol. 1, Chalmers, J.M. and Griffiths, P.R. (Eds.), John Wiley and Sons, Chichester, pp. 141-149, 2002.
(69) Werninghaus, T., Friedrich, M., Hahn, J., Richter, F., and Zahn, D.R.T., *Diamond Relat. Mater.*, 6, 612 (1997).
(70) Djaoued, Y., Bruning, R., Bersani, D., Lottici, P.P., and Badilescu, S., *Mater. Lett.*, 58, 2618 (2004).
(71) Darimont, G.L., Gilbert, B., and Cloots, R., *Mater. Lett.*, 58, 71 (2004).
(72) Portinha, A., Teixeira, V., Carneiro, J., Beghi, M.G., Bottani, C.E., Franco, N., Vassen, R., Stoever, D., and Sequeira, A.D., *Surf. Coat. Technol.*, 188-189, 120 (2004).
(73) Teixeira, V., Andritschky, M., Fischer, W., Buchkremer, H.P., and Stover, D., *J. Mater. Proc. Technol.*, 92-93, 209 (1999).
(74) Campion, A. and Kambhampati, P., *Chem. Soc. Rev.*, 27 (1998).
(75) Smith, W.E. and Rodger, C., in *Handbook of Vibrational Spectroscopy*, Vol. 1, Chalmers, J.M. and Griffiths, P.R. (Eds.), John Wiley and Sons, Chichester, pp. 775-784, 2002.
(76) Babic, R. and Metikos-Hukovic, M., *Thin Solid Films*, 359, 88 (2000).
(77) Graff, M., Bukowska, J., and Zawada, K., *J. Electroanal. Chem.*, 567, 297 (2004).
(78) Huynh, N., Bottle, S.E., Notoya, T., and Schweinsberg, D.P., *Corros. Sci.*, 44, 2583 (2002).
(79) McAnnally, G.D., Everall, N.J., Chalmers, J.M., and Smith, W.E., *Appl. Spectrosc.*, 57, 44 (2003).
(80) Campion, A., *Ann. Rev. Phys. Chem.*, 36, 549 (1985).